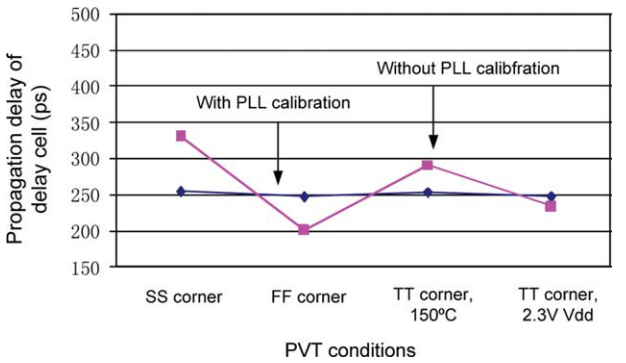

Figure 6 Simulated delay of the proposed delay cell with and without PLL calibration. [Color figure can be viewed in the online issue, which is available at wileyonlinelibrary.com]

be achieved by setting different divider ratios between the ring oscillator frequency and reference frequency. In this design, the tuning range of the ring oscillator in the PLL was measured to be from 60 to 180 MHz, which means that the delay of the single delay cell can be adjusted from 138 ps to 417 ps. Due to the experiment limitation, the delay is only measured for the TT corner and room temperature. However, the wide tuning range of the delay cell from the measurement results indicates that the delay cell is able to accommodate fairly large PVT changes. Figure 6 gives the simulation results for the delay of the proposed delay cell with and without PLL calibration over different PVT conditions. It can be seen that, with the use of the PLL, the proposed delay cell is capable of calibrating its delay to around 250 ps regardless of the PVT conditions.

4. CONCLUSIONS

We proposed and implemented a novel PLL based close-loop tunable delay generator on a 0.18-μm CMOS process for UWB and time-domain RF applications. The relative delay error of less than 0.8% has been demonstrated. The delay generator is functional for arbitrary digital clock regardless its frequency, slope, coding scheme, and duty cycle. The generated delay is able to conduct self-correction against PVT variation through a negative feedback loop. With scaling-down CMOS processes, the minimum delay resolution could be further reduced. The proposed delay generator is suitable for applications where short delay, such as pulse-width control and pulse position modulation for UWB systems, is desired. In applications which require longer delay like short-range radar, digital counter based delay generators are more efficient.

ACKNOWLEDGMENTS

This work was supported in part by the National Science Foundation, Air Force Research Laboratory, and the US Army.

REFERENCES

1. I. Guvenc and H. Arslan, Performance evaluation of UWB system in the presence of timing jitter, In: Proceedings of the 2003 IEEE Conference on Ultra Wideband Systems and Technologies, 2003, pp. 136–141.
2. S. Tiuraniemi, CMOS pulse generator design for TH-PPM UWB system, Presented at the Finnish Wireless Communications Workshop 2003, Oulu, Finland, 2003, pp. 136–139.
3. C. Kim,J. Yang,D. Kim, and S. Hong, A K-band CMOS voltage controlled delay line based on an artificial left-handed transmission line, IEEE Microwave Wireless Compon Lett 18 (2008), 731–733.
4. J. Schwartz,I. Arnedo,M. Laso,T. Lopetegi,J. Azana, and D. Plant, An electronic UWB continuously tunable time-delay system with nanosecond delays, IEEE Microwave Wireless Compon Lett 18 (2008), 103–105.
5. D. Borg and D.B. Hunter, Tunable microwave photonic passive delay line based on multichannel fibre grating matrix, Electron Lett 41 (2005), 537–538.
6. J.L. Rossello and J. Segura, An analytical charge-based compact delay model for submicrometer CMOS inverters, IEEE J Solid State Circuits 51 (2004), 1301–1311.
7. D. Auvergne,J.M. Daga, and M. Rezzoug, Signal transition time effect on CMOS delay, IEEE Trans Circuits Syst I Fundam Theory Appl 47 (2000), 1369–1369.

EXPERIMENTAL DEMONSTRATION OF AN ULTRAFAST ALL-OPTICAL BIT-ERROR INDICATING SCHEME

C. Finot and J. Fatome
Laboratoire Interdisciplinaire CARNOT de Bourgogne, UMR 5209 CNRS-Université de Bourgogne, 9 Av. A. Savary, BP 47 870, 21078 DIJON Cedex, France; Corresponding author: christophe.finot@u-bourgogne.fr

Received 10 May 2010

ABSTRACT: *We experimentally demonstrate an all-optical bit error monitoring scheme based on the self-phase modulation occurring during the propagation in a highly nonlinear fiber followed by an optical bandpass filter. Numerical simulations are confirmed by experimental observations performed at a repetition rate of 40 Gb/s.* © 2010 Wiley Periodicals, Inc. Microwave Opt Technol Lett 53:392–395, 2011; View this article online at wileyonlinelibrary.com. DOI 10.1002/mop.25711

Key words: *nonlinear optics; all-optical processing; self-phase modulation; bit-error indicating scheme*

1. INTRODUCTION

With the advent of high-speed optical transmissions (40 Gb/s and beyond) and the increasing complexity of photonic networks, it becomes more and more crucial to develop adequate means to suitably characterize the quality of the optical data stream. Therefore, optical performance monitoring has become a very active field [1] that has recently stimulated intense research to overcome the bandwidth limitations of the usual electronics. The main target is to better detect and control the various impairments (noise, dispersion fluctuations, polarization mode dispersion etc.) that negatively impact the quality of service. In this context, any optical device that can highlight in real time the pulses responsible for detection error is highly desirable for improved fault management [2, 3].

In this article, we experimentally demonstrate such a device. More precisely, based on the idea initially suggested by Oda and Maruta [4] and the related numerical investigation done by Zhang et al. [3], we confirm that the nonlinear response of optical fibers combined with an adequate optical spectral filtering can provide an efficient way to discriminate well-defined ''0'' or ''1'' bits of information from potential errors. We will first describe and illustrate the experimental set-up and the principle of operation of the device that we have implemented. Proof-of-

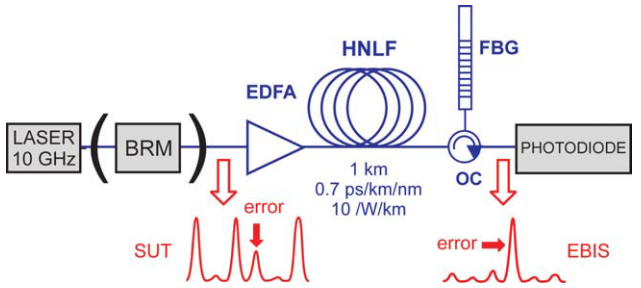

Figure 1 Experimental set-up. [Color figure can be viewed in the online issue, which is available at wileyonlinelibrary.com]

principle experiments carried out at 40 Gb/s will fully confirm the behavior predicted by numerical simulations.

2. EXPERIMENTAL SET-UP

The configuration we investigate is sketched in Figure 1. The experimental set-up relies exclusively on commercially available components commonly used for optical telecommunications. A low jitter fiber laser source is actively mode-locked by a 10-GHz RF signal and delivers Fourier-transform-limited picosecond pulses (2 ps, such a temporal duration is compatible with 160 Gb/s telecommunication). A x4 bit rate multiplier (BRM) is used to simulate the basic degraded 40 GHz return-to-zero pulse sequence with various levels that will constitute the signal under test (SUT). The resulting signal is sent into an erbium-doped fiber amplifier with a moderate output average power. The amplified pulse train then propagates into a highly nonlinear fiber (fiber from ofs specialty photonics division). This fiber is 920 meter long and presents a low anomalous dispersion (D = 0.7 ps/km/nm) combined with a high value of nonlinearity (10/W/km). The linear losses and dispersion slope are both reduced (0.6 dB/km and 0.01 ps^2/km/nm, respectively). The nonlinearity of the fiber leads to an intensity-dependent spectral expansion of the pulses due to self-phase modulation [4, 5]. At the output of the fiber, an optical bandpass filter made of a fiber Bragg grating associated with an optical circulator is used to carve into the expanded spectrum. The central wavelength of this filter is the same as the original stream, and its spectral width is 200 GHz. The resulting error bit indicating signal (EBIS) is analyzed by means of a usual photodetector combined with a high-speed digital sampling oscilloscope (50 GHz optical bandwidth).

3. PRINCIPLE OF OPERATION

The key element in this set-up is the optical transfer function (TF) that links the input and output powers. According to the choice of parameters of the fiber and the filter, the TF shape may significantly vary [6]. Indeed, the architecture described in Figure 1 is well-known in the context of optical regeneration [6–9], in which the aim is not to facilitate the detection of errors but to limit output pulse train jitter and act as an all-optical power limiter: this requires a TF with a large plateau characterized by an inflexion point. Another application based on similar architecture has also been recently proposed and targets the all-optical magnification of amplitude jitter [10]. Our purpose is here very different from optical regeneration or optical magnification so that the requirements on the TF differ significantly. More precisely and as it can be seen in Figure 2, the TF needs to exhibit a nonmonotonous behavior characterized by two local minima (initial powers 0 and 12 mW) having an output value close to zero. A maximum of the TF should be observed for powers near the middle of the two minima (around 7 mW in our case).

The principle of the device can then be easily understood as follows [3, 4]: by properly adjusting the peak power of the "1" bits so as to be close to the second minima of the TF, the pulses emerging from the bit error indicating scheme will have a very low output level. On the contrary, the pulses having a peak power that may lead to a detection error fall in the range neighboring the maximum of the TF. Consequently, they will exhibit a high output level and will be straightforwardly detected.

Let us note that the experimental scheme that we have implemented could have been replaced by other well-documented fibered systems presenting similar nonmonotonous TF. For example, alternatives based on Mamyshev-regenerator like schemes (MR) [11–14] or on nonlinear optical loop mirror (NOLMs) [15] could be considered. Let us, however, point out that in the case of the MR which is based on a very similar physical principle (self-phase modulation in an optical fibre, but operating in the normal dispersion regime and with an offset filtering), the required input power will be significantly higher and the process may additionally induce some detrimental timing jitter as well as pulse-to-pulse interaction, which may complexify the detection process [6, 16, 17]. Regarding the use of a NOLM, such a solution will not be appropriate: contrary to the proposed scheme or to MR, NOLMs are sensitive to the instantaneous power and not to the peak-power of the pulse.

4. NUMERICAL SIMULATIONS

To test the viability of the proposed approach, we have run some preliminary numerical simulations. The device under investigation can be modelled by the well-known nonlinear Schrödinger equation [5, 6] in such a way that the TF can be predicted. Figure 2 highlights the remarkable agreement achieved between the numerical simulations (solid grey line) and the experimental results (black circles). Based on this accurate model, we can test the ability of the device to efficiently detect the potential errors. Therefore, a realistic sequence of 16 bits (return-to-zero format) is plotted in Figure 3 (a). The SUT is made of Gaussian pulses and presents a finite extinction ratio (linked to a finite extinction ratio of an initial modulator or to the growth of ghost pulses during the transmission [18]), fluctuations in the "1" power as well as a potential error. After the nonlinear device [Fig. 3(b)], both "1" bits and "0" bits present

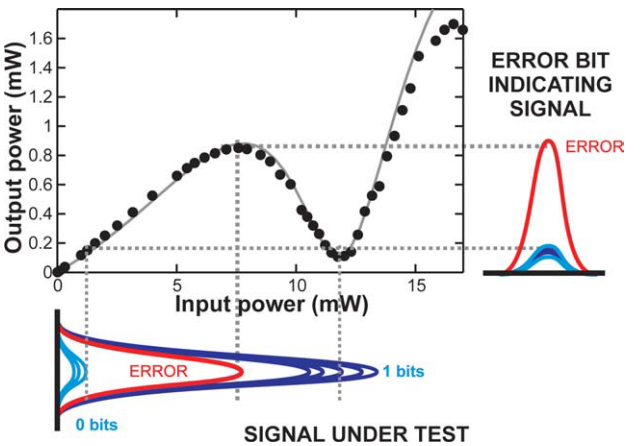

Figure 2 Transfer function of the proposed device. Experimental results (black circles, results obtained at a repetition rate of 10 Gbps) are compared with the numerical predictions based on the nonlinear Schrödinger equation (solid grey line). [Color figure can be viewed in the online issue, which is available at wileyonlinelibrary.com]

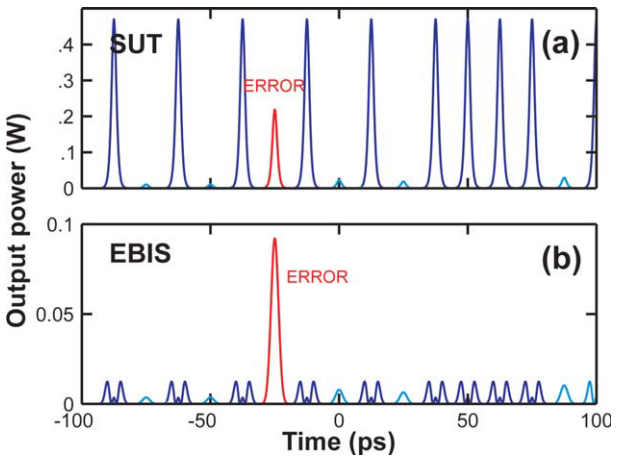

Figure 3 Numerical simulations. The SUT containing a potential error (subplot a) is compared with the EBIS (subplot b). [Color figure can be viewed in the online issue, which is available at wileyonlinelibrary.com]

a reduced level, whereas the error pulse has a significantly enhanced level. More careful inspection of the EBIS reveals that the output "1" state exhibits a double peak structure, but as no relevant measurement is carried out on those pulses, this does not constitute any drawback.

5. EXPERIMENTAL RESULTS

To experimentally simulate a given sequence including an error, we have used the BRM and starting from a 10 GHz pulse train, we have obtained a 40 GHz pulse trains with various peak-power levels. Two sequences have been tested. The first sequence, plotted in Figure 4 (a1), presents some undesirable pulses in the "0" bits slots, which level could potentially lead to detection errors. In Figure 4(a2), at the output of our device, the outcoming stream reveals that the errors become readily apparent. The level of the "1" state is indeed significantly reduced. The ability of the device to conveniently deal with low level pulses, typically ghost pulses [18], is clearly reflected in the second sequence [Figs. 4(b1) and 4(b2)]. As a consequence,

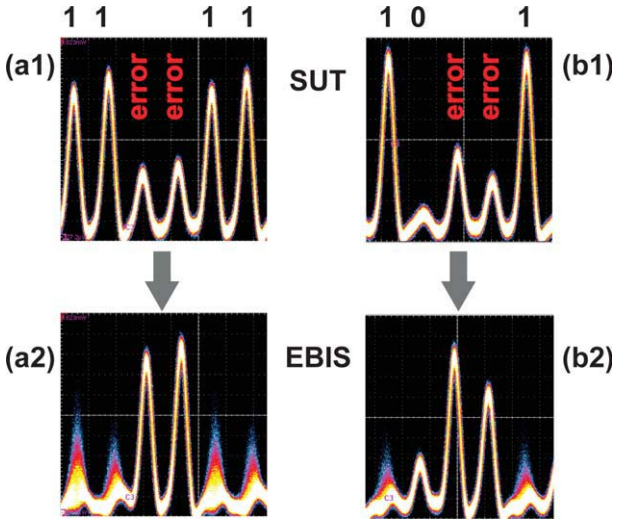

Figure 4 Experimental results. Input (subplots 1) and output (subplots 2) pulses are compared for two sequences (subplots a and b). [Color figure can be viewed in the online issue, which is available at wileyonlinelibrary.com]

only one judge threshold is necessary to analyze the EBIS and to identify the potential errors. Less importantly, one can also notice from the various experiments that, in the EBIS, "1" bits are affected by a much higher jitter than the "0" bits, which is consistent with the regime of amplitude jitter magnification [10]. Moreover, the previously mentioned double peaked structure can be guessed.

6. CONCLUSIONS

We have experimentally demonstrated an easy-to-implement and cost-effective device able to discriminate the undesirable pulses that may potentially compromise the detection from the "0" and "1" pulses having a regular level. The proposed all-optical function benefits from the quasi-instantaneous response of the Kerr non-linearity of optical fibers. Our experimental results obtained at a repetition rate of 40 Gb/s can, therefore, be in principle extended to any higher repetition rates (100 Gb/s or even 160 Gb/s [7]). Measurements have been made on a single channel configuration, but using a counter-propagating configuration [19] or using polarization multiplexing [14], one can enable to handle as much as four different wavelengths simultaneously.

ACKNOWLEDGMENTS

This research was supported by the Agence Nationale de la Recherche (FUTUR project: ANR-06-TCOM-016, PERSYST 2 project: ANR-07-TCOM-014) and by the Conseil Regional de Bourgogne.

REFERENCES

1. Z. Pan, C. Yu, and A.E. Willner, Optical performance monitoring for the next generation optical communication networks, Opt Fiber Technol 16 (2010), 20–45.
2. L.Y. Chan, K.K. Qureshi, P.K.A. Wai, B. Moses, L.F.K. Lui, H.Y. Tam, and M.S. Demokan, All-optical bit-error monitoring system using cascaded inverted wavelength converter and optical nor gate, IEEE Photon Technol Lett 15 (2003), 593–595.
3. Z. Zhang, X. Zhou, R. Liang, Z. Qin, and Y. Liu, An all-optical bit-error indicating scheme based on self-phase modulation and filtering, Opt Commun 282 (2009), 3163–3167.
4. S. Oda and A. Maruta, Two-bit all-optical analog-to-digital conversion by filtering broadened and split spectrum induced by soliton effect or self-phase modulation in fiber, IEEE J Sel Top Quantum Electron 12 (2006), 307–314.
5. G.P. Agrawal, Nonlinear fiber optics, 4th ed., Academic Press, San Francisco, CA, 2006.
6. J. Fatome and C. Finot, Scaling guidelines of a soliton-based power limiter for 2r-optical regeneration applications, 11th International Conference on Transparent Optical Networks, IEEE, 2009, pp. 1303–1306.
7. T. Ohara, H. Takara, S. Kawanishi, T. Yamada, and M.M. Fejer, 160 gb/s all-optical limiter based on spectrally filtered optical solitons, IEEE Photon Technol Lett 16 (2004), 2311–2313.
8. M. Asobe, A. Hirano, Y. Miyamoto, K. Sato, K. Hagimoto, and Y. Yamabayashi, Noise reduction of 20 gbit/s pulse train using spectrally filtered optical solitons, Electron Lett 34 (1998), 1135–1136.
9. M. Gay, M. Costa e Silva, T.N. Nguyen, L. Bramerie, T. Chartier, M. Joindot, J.C. Simon, J. Fatome, C. Finot, and J.L. Oudar, 170 gbit/s bit error rate assessment of regeneration using a saturable absorber and a nonlinear fiber based power limiter, IEEE Photon Technol Lett 22 (2010), 158–160.
10. J. Fatome and C. Finot, All-optical fiber-based amplitude jitter magnifier, 12th International Conference on Transparent Optical Networks, IEEE, 2010.
11. P.V. Mamyshev, All-optical data regeneration based on self-phase modulation effect, European Conference on Optical Communication, ECOC'98, 1998, pp. 475–476.

12. X. Zhang, X.M. Ren, N. Zhao, Y. Wang, L. Zheng, and Y. Huang, Extinction ratio enhancement of self-phase modulation based all-optical regenerated signals in microstructuted fibers, Microwave Opt Technol Lett 52 (2010), 347–351.
13. Y. Yang and C. Lou, Experimental investigation of the influence of filters on regeneration performance in self-phase modulation based regenerator, Microwave Opt Technol Lett 49 (2007), 192–195.
14. T. Ohara, H. Takara, A. Hirano, K. Mori, and S. Kawanishi, 40 gb/s x 4 channel all-optical multichannel limiter utilizing spectrally filtered optical solitons, IEEE Photon Technol Lett 15 (2003), 763–765.
15. S. Boscolo, S.K. Turitsyn, and K.J. Blow, Nonlinear loop mirror-based all-optical signal processing in fiber-optic communications, Opt Fiber Technol 14 (2008), 299–316.
16. C. Finot, T.N. Nguyen, J. Fatome, T. Chartier, L. Bramerie, M. Gay, S. Pitois, and J.C. Simon, Numerical study of an optical regenerator exploiting self-phase modulation and spectral offset filtering at 40 gbit/s, Opt Commun 281 (2008), 2252–2264.
17. L. Provost, C. Finot, K. Mukasa, P. Petropoulos, and D.J. Richardson, Design scaling rules for 2r-optical self-phase modulation-based regenerators 2r regeneration, Opt Express 15 (2007), 5100–5113.
18. P.V. Mamyshev and N.A. Mamysheva, Pulse-overlapped dispersion-managed data transmission and intrachannel four-wave mixing, Opt Lett 24 (1999), 1454–1546.
19. L. Provost, F. Parmigiani, C. Finot, K. Mukasa, P. Petropoulos, and D.J. Richardson, Analysis of a two-channel 2r all-optical regenerator based on a counter-propagating configuration, Opt Express 16 (2008), 2264–2275.

DESIGN OF HIGH-EFFICIENCY AND BROADBAND-TUNED CLASS AB POWER AMPLIFIER

Aynaz Vatankhahghadim and Slim Boumaiza
Department of Electrical and Computer Engineering, EmRG Group, University of Waterloo, Waterloo, Canada; Corresponding author: aynaz.vatankhah@gmail.com or avatankh@engmail.uwaterloo.ca

Received 10 May 2010

ABSTRACT: *The design of broadband matching networks (MNs) exploiting filter theory is presented in this article for synthesizing broadband and highly efficient power amplifiers (PAs). Starting from sets of optimum impedances over the design frequency (obtained from load/pull measurement), the MNs are designed using a systematic approach. The impact of the second harmonic termination on the transistor performance is investigated and used to optimize the power efficiency over broad frequency range. Two PAs were designed with the proposed methodology using 25-W GaN device. The designs targeted the frequency bands of 1.8–2.2 GHz (20% BW) and 1.8–2.7 GHz (40% BW). The former achieved the drain efficiency (DE) of about 70% and output power of 45.5 dBm (±1 dB), whereas the latter delivered a DE of about 60% and output power of 45.5 dBm.* © 2010 Wiley Periodicals, Inc.
Microwave Opt Technol Lett 53:395–398, 2011; View this article online at wileyonlinelibrary.com. DOI 10.1002/mop.25710

Key words: *broadband; high-efficiency power amplifier; class AB*

1. INTRODUCTION

Wireless communications have been continuously evolving to meet the user's diverse needs. In this regard, several wireless standards are either currently deployed or will be introduced in the near future. Service providers have to cope with multiple protocols as the different standards will need to coexist. To deal with multiple standards, several solutions can be considered such as multiple radios, multiband radios, and broadband ones. Using multiple radios to cover the multiple standards is a costly, large, and nonoptimal solution. However, multiband and broadband structures make use of one radio that meets the needs of multiple standards. In other words, multiband systems work for multiple, discrete, and narrowband frequency intervals (usually far from each other), whereas broadband structures aim for a single but broader frequency range trying to target at least two wireless standards. The main challenge of the design of multiband/broadband power amplifier (PA) is to maintain as good RF performance compared with narrowband PA.

PA is one of the important building blocks of the wireless systems, which is frequency dependent, because its performance degrades as the frequency moves away from the design frequency. Therefore, advanced multiband/broadband methodologies are needed to develop multiband/broadband PAs. Several attempts are reported in the literature covering the design of broadband PAs using different device technologies and targeting different specifications such as output power and bandwidth. For instance, targeting 0.5–2.5 GHz, a single-stage GaN PA is designed, achieving saturated output power of +41 dBm and drain efficiency (DE) of 46% [1]. Colantonio et al. [2] used nonlinear CAD approach to design broadband PA targeting frequencies of 0.8–4 GHz, which resulted in an average DE of about 50% with an output power higher than 32 dBm. A class J PA targeting 1.35–2.25 GHz (50%) was designed delivering 10-W output power with the DE of about 60–70% [3]. Although this amplifier operates over broad bandwidth with fairly good efficiency, there is no systematic methodology followed by the designer for broadband design.

In this article, a design methodology of broadband PA with optimized power performance over the bandwidth is developed. Taking into account for device characteristics such as optimum load and source impedances (using large-signal model of the transistor), corresponding matching networks (MNs) are designed to present the right impedances to the transistor over the bandwidth. The high-efficiency broadband PAs are designed and fabricated for 1.8–2.2 and 1.8–2.7 GHz.

2. BROADBAND MN DESIGN METHODOLOGY

Designing a PA consists of three main steps: determination of optimum source and load impedances, design of input and output MN, and design of bias network. To design the MNs, after obtaining optimum load and source impedances, proper topologies and methodologies should be used.

There are several broadband methodologies such as multi L-section, multisection quarter-wave transformers, and tapered transmission lines [4]. In this article, multi L-section transformation for complex loads is used to design the broadband MN as it is the most suitable approach for complex to real impedance conversion. This approach can be applied for any targeted bandwidth as long as the resulting J-inverters are kept within reasonable range. More details of this method are given in the following paragraph.

Multi L-section transformation for complex load is based on Chebychev filter theory [5, 6]. In this method, reactive part of the source/load impedance is considered as the first element of the filter. Given the reactive part of the source/load, a decrement factor δ is calculated using (1) [5]:

$$\delta = \frac{1}{g_0 g_1 \omega_1'} = \frac{1}{G_0' L_1' \omega_1'} = \frac{1}{R_0' C_1' \omega_1'} \tag{1}$$

in which ω_1' is the cutoff frequency.